Research Square

Preprints are preliminary reports that have not undergone peer review.
They should not be considered conclusive, used to inform clinical practice,
or referenced by the media as validated information.

Research on Core Loss Prediction Models and Multi-Condition Optimization Based on Data-Driven Methods

Yaoyang Cai

438123387@qq.com

Research Article

Keywords: core loss, steinmetz equation, excitation waveform classification, magnetic flux density, machine learning

Posted Date: November 24th, 2026

DOI: https://doi.org/10.21203/rs.3.rs-11708875/v1

License: This work is licensed under a Creative Commons Attribution 4.0 International License.
Read Full License

Research on Core Loss Prediction Models and Multi-Condition Optimization Based on Data-Driven Methods

Yaoyang Cai [a*]

[a] *School of Northeastern University, Shenyang, 110819, China;*

[*] *Corresponding authors' E-mail addresses: 43812387@qq.com (Yaoyang Cai).*

Abstract

As a core component in power conversion equipment, the core loss characteristics of magnetic components have a direct impact on the overall operational efficiency of power electronic systems. Under non-sinusoidal excitation conditions such as triangular and trapezoidal waves, as well as under dynamic temperature variations, the loss prediction error of the traditional Steinmetz empirical equation is relatively large. To address the limitations of traditional loss models in prediction accuracy, this paper first extracts relevant feature parameters based on flux density data and constructs an excitation waveform classification model; subsequently, temperature variables are introduced into the Steinmetz equation to propose a modified Steinmetz equation; on this basis, a data-driven method is used to achieve high-precision prediction of core losses; finally, to balance magnetic energy transfer characteristics, the trained neural network model is coupled with an improved particle swarm optimization algorithm, taking both core loss minimization and magnetic energy transfer maximization as dual optimization objectives, and parameter optimization under constraints is conducted. The research results show that the modified Steinmetz equation achieves a goodness of fit (R^2) of 0.9908, and compared to the original model, its loss prediction capability under variable temperature conditions is significantly improved; the neural network model achieves a goodness of fit (R^2) of 0.9982 and a mean squared error (MSE) of 134,018.16 on the test set; after optimization with the coupled improved particle swarm algorithm, the optimal parameter combination balancing low core losses and high magnetic energy transfer characteristics is obtained.

Keywords: core loss, steinmetz equation, excitation waveform classification, magnetic flux density, machine learning.

1. Introduction

With the continuous innovation of modern power electronics technology, electric energy conversion technology has been widely integrated into various fields such as new energy, communications, rail transportation, and electric vehicles, showing a significant growth trend in the demand for power converters [1], [2], [3]. As a key component of power converters, magnetic components undertake core functions such as magnetic energy transfer, storage, and filtering, and their performance directly constrains the system's size, weight, power loss, and manufacturing cost.[4], [5], [6]. Under high-frequency operating conditions, core loss constitutes the dominant portion of the total loss of magnetic components and exhibits a complex coupling relationship with multiple factors, including frequency, magnetic flux density, temperature, and excitation waveform, showing significant nonlinear characteristics and interactive effects [7]. Existing magnetic core loss models still have considerable limitations in prediction accuracy and are difficult to meet the engineering requirements of modern high-frequency, high-power-density application scenarios.

With the continuous improvement of operating efficiency, power supply stability, and device power density requirements in power systems, the loss characteristics of magnetic components, particularly hysteresis loss, directly affect the energy efficiency and operational reliability of power electronic equipment, becoming a key issue that urgently needs to be addressed in the optimized design of magnetic devices [8], [9]. The Steinmetz Equation (SE), as a classical empirical model for the quantitative calculation of core losses, provides a foundational framework for the engineering estimation of magnetic losses [10]. However, this equation is only applicable under narrow operating conditions with sinusoidal magnetic flux excitation, no DC bias, and constant temperature. It lacks the ability to represent the coupled effects of temperature, DC bias, and excitation waveform, its fitting parameters have a limited applicable range, and its physical mechanism explanation is insufficient, making it difficult to meet the loss assessment requirements of power electronic equipment under complex real-world operating conditions.

In order to overcome the engineering applicability limitations of the classical equation, the academic community has successively proposed various improved loss calculation models. Early modification approaches, represented by the Modified Steinmetz Equation (MSE), extend the model's applicability to non-sinusoidal excitation scenarios by introducing an integral term of the rate of change of instantaneous magnetic flux density, thereby improving the accuracy of loss prediction under typical excitation conditions such as square waves and pulse waves to some extent. Subsequently, the Generalized Steinmetz Equation (GSE) and the improved Generalized Steinmetz Equation (iGSE) further optimize the physical expression logic of loss calculation based on the transient characteristics of magnetic flux density waveforms, demonstrating more robust predictive

performance under regular non-sinusoidal excitation conditions [11] [12]. Li et al. [13] proposed the GSE to describe the relationship between losses and the rate of change of magnetic flux density, enhancing prediction accuracy under non-sinusoidal waveforms. Venkatachalam et al. [14] proposed the iGSE, introducing a recursive algorithm to separate the primary and secondary hysteresis loops and calculate the losses separately. This method achieves higher accuracy and broader applicability under non-sinusoidal excitations. A. Arruti [15], based on the iGSE, developed the composite improved generalized Steinmetz equation (ciGSE), achieving high-precision predictions over the full duty cycle range under triangular wave excitations. Large-scale experimental verification showed that the overall root mean square error (RMSE) was reduced to 10.02%. Although analytical models feature good physical interpretability, their empirical parameters need calibration for different materials, and their predictive accuracy and generalization capability remain limited under complex waveforms and multiple operating conditions. To improve the prediction accuracy of core losses, Shuai Chunyan et al. [16], on the basis of the Steinmetz equation, used data analysis methods to estimate the impact mechanism of temperature on core loss variation, subsequently incorporating the temperature variable into the Steinmetz equation and proposing a parameter optimization method for the improved Steinmetz equation based on the simplex method. By comparing the results of error loss functions with optimal parameter outcomes, the reasonableness and robustness of the temperature-modified Steinmetz equation were verified. Finally, sensitivity analysis confirmed the positive role of introducing the temperature variable in enhancing the importance and accuracy of the Steinmetz equation output results. However, this study did not take the impact of continuous temperature changes on core loss into account. Moreover, most of these modified models assume a constant temperature as a basic premise and do not incorporate the effect of temperature on core material permeability, coercivity, and loss coefficients into a unified modeling framework. When converters operate under wide temperature range conditions (such as in automotive electronics or outdoor renewable energy equipment), the coupling effect of ambient temperature and device self-heating can lead to significant deviations in core loss characteristics, causing substantial predictive errors for correction models that rely on room-temperature calibrated parameters in practical applications. Wang Ning et al. [17] proposed a Steinmetz loss prediction model considering temperature effects for nanocrystalline materials. Within the temperature range of 25~125°C, this model first linearly adjusts the peak magnetic flux density Bm in the classical equation using the temperature variable, and then introduces a temperature-related term to characterize its nonlinear correlation with core loss. However, this approach significantly increases the complexity of model solution.

With the rise of data-driven approaches and their broad applicability in various engineering fields, some studies have begun introducing machine learning methods into the field of magnetic core loss prediction. J. He et al. [18] conducted a comparative study of multiple machine learning and deep learning models regarding core loss prediction performance under different material and waveform conditions. The results indicate that in complex nonlinear scenarios, deep neural networks demonstrate superior predictive capability. Deng, J et al. [19] proposed a magnetic core loss modeling method based on Knowledge-Aware Artificial Neural Networks (KANN), embedding iGSE into the neural network architecture, thereby improving prediction accuracy and computational efficiency. Solimene, L et al. [20] constructed a hybrid modeling approach combining physical cognition and machine learning to predict magnetic core losses based on the MagNet dataset. Shen X et al. [21] proposed a magnetic core loss estimation method based on Deep Neural Networks (DNN). This method achieves high-precision prediction under high-frequency conditions up to 1 MHz by optimizing the network structure, with high-frequency errors below 1%. P. Brendel et al. [22] addressed the insufficient computational efficiency of traditional physical models in magnetic core loss prediction by combining Convolutional Neural Networks (CNN) with Physics-Informed Neural Networks, proposing a ConvPINN hybrid modeling approach. By embedding physical laws as prior constraints into the neural network training process, this method significantly enhances the computational efficiency of magnetic core loss while maintaining predictive accuracy. Luo Pengyong et al. [23] proposed a multi-feature magnetic core loss prediction model integrating Temporal Convolutional Networks (TCN) with attention mechanisms. This model demonstrates good stability and compressibility under small-sample conditions and out-of-distribution temperature scenarios, and relevant experiments have verified its effectiveness and feasibility for magnetic core loss assessment under complex operating conditions. However, the study lacks systematic verification regarding its applicability across a wider temperature range and frequency spectrum.

Under this background, this study offers the following main contributions: (1) Extract time-domain statistical features and differential features of magnetic flux density, and use a random forest algorithm to achieve intelligent recognition of three types of excitation waveforms. (2) Introduce a temperature polynomial to modify the Steinmetz equation and construct a neural network surrogate model to achieve high-precision prediction of core losses. (3) Couple the trained neural network model with the improved particle swarm optimization algorithm, with the objectives of minimizing core loss and maximizing transmitted magnetic energy, to carry out parameter optimization under multi-objective constraints.

Based on this, this paper focuses on the high-precision prediction of magnetic core losses and multi-condition optimization under wide temperature ranges and complex excitation waveforms. The overall research framework is as follows: Firstly, waveform features are extracted from the measured magnetic flux density sequences, and a random forest classification model is constructed to achieve automatic recognition of different excitation waveforms, providing a basis for subsequent scenario-specific modeling. Secondly, the temperature variable is introduced into the classical Steinmetz equation to establish a loss calculation model considering temperature correction, thereby improving the analytical prediction accuracy under variable temperature conditions. On this basis, by integrating multidimensional features such as waveform classification results, temperature, frequency, and magnetic flux density, a BP neural network loss prediction model is built to achieve high-precision prediction of magnetic core losses under complex conditions. Finally, the trained neural network prediction model is coupled with an improved particle swarm optimization algorithm, with the optimization goal of minimizing magnetic core loss and maximizing transmitted magnetic energy, to perform constrained optimization and obtain the optimal parameter combination that balances both energy efficiency and transmission capacity, providing theoretical guidance and methodological support for the optimization design of high-frequency magnetic components.

2. Data Sources and Processing

2.1 Data Sources

This study's dataset comes from the 2024 China Graduate Mathematical Modeling Competition, Problem C, and includes four types of magnetic materials, labeled Material 1, Material 2, Material 3, and Material 4.

Table 1. Data amount provided for each material.

Material	Excitation Waveform	Data Amount
Material 1	Sinusoidal wave	1067
	Triangular wave	1412
	Trapezoidal wave	921
Material 2	Sinusoidal wave	1097
	Triangular wave	1003
	Trapezoidal wave	900
Material 3	Sinusoidal wave	1010
	Triangular wave	1078
	Trapezoidal wave	1112
Material 4	Sinusoidal wave	1067
	Sinusoidal wave	1412
	Sinusoidal wave	921

For each type of material, the data recorded contains physical quantities such as temperature (T), frequency (F), magnetic flux density (B), iron loss (y), and excitation waveform, each represented by 1,024 sampling points. The number of samples for each material is detailed in Table 1. Data was collected under four temperature conditions: 25 °C, 50 °C, 70 °C, and 90 °C. Excitation waveforms include sine, triangle, and trapezoid waves. There are no missing values or abnormal samples in this dataset, which is split into training and test sets with an 80:20 ratio.

2.2 Data preprocessing and feature extraction

Core loss is a key performance indicator of magnetic components, and the excitation waveform directly affects how the magnetic flux density changes over time[24]. The rise and decay patterns of the flux density vary under different waveforms, which in turn leads to different core losses. Therefore, we first analyzed the flux density waveforms, randomly selecting flux density samples with different waveform labels in equal amounts by category, and plotted the changes in flux density over time within a single cycle, as shown in **Fig. 1**.

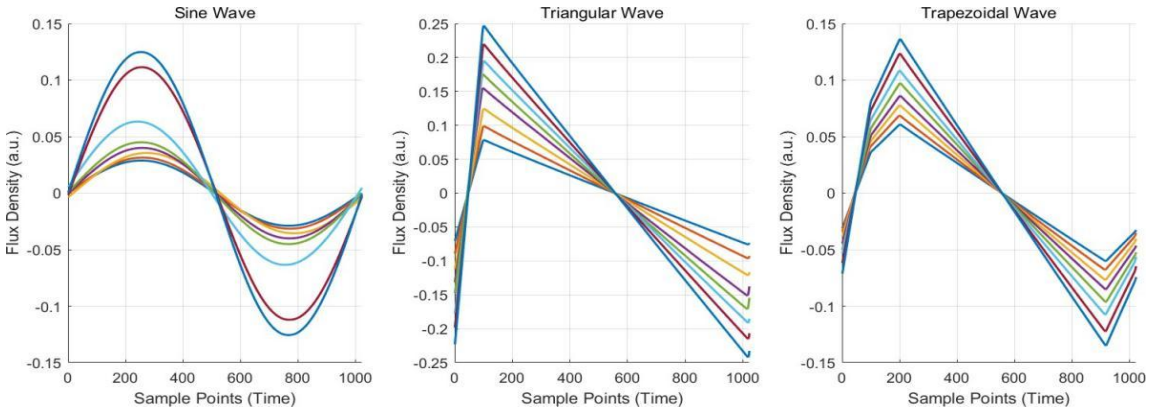

Fig. 1. The variation of magnetic flux density over time.

As shown in **Fig. 1**, By observing waveform patterns, in order to effectively extract feature quantities that reflect waveform characteristics, a graphical analysis of flux density-related statistics is conducted. The selected statistics include maximum and minimum values, mean, standard deviation, peak-to-peak value, as well as the mean and standard deviation of first-order and second-order differences.

For a given time series B = [B_1, B_2, ..., B_n], the first-order difference is expressed as:

$$\Delta B_i = B_{i+1} - B_i \tag{1}$$

Where ΔB_i is the difference between adjacent elements in the time series.i=1,2...,n-1

The formula for calculating the mean of first-order differences is:

$$\mu\Delta B = \frac{1}{n-1}\sum_{i=1}^{n-1}\Delta B_i \tag{2}$$

The formula for calculating the standard deviation of the first-order difference is:

$$\sigma\Delta B = \sqrt{\frac{1}{n-2}\sum_{i=1}^{n-1}(\Delta B_i - \mu\Delta B)^2} \tag{3}$$

The second-order difference is expressed as the difference between first-order differences, defined as:

$$\Delta^2 B_i = B_{i+1} - B_i \tag{4}$$

The formula for calculating the mean of the second-order difference is:

$$\mu\Delta^2 B = \frac{1}{n-2}\sum_{i=1}^{n-2}\Delta^2 B_i \tag{5}$$

The formula for calculating the standard deviation of the second-order difference is:

$$\sigma\Delta^2 B = \sqrt{\frac{1}{n-3}\sum_{i=1}^{n-2}(\Delta^2 B_i - \mu\Delta^2 B)^2} \tag{6}$$

Based on the above statistical characteristics, draw feature statistical charts of different waveforms, as shown in **Fig. 2**. Then, combined with the comparison between statistics, as shown in **Fig. 3 Fig. 4 Fig. 5 .**From the comparison results of the above statistical measures, it is evident that different waveform types exhibit significant differences in their distribution within the feature space. Accordingly, this study selected the maximum, minimum, mean, standard deviation, peak-to-peak value, as well as the mean and standard deviation of the first-order and second-order differences as feature variables. The aforementioned features can effectively distinguish various excitation waveforms: the sine wave shows smooth and continuous variation characteristics, whereas the trapezoidal wave exhibits stage-like changes with distinct rising and falling segments. The overall classification accuracy of the test set reached 99.84%, with the sine wave being identified with 100% accuracy; a few misclassifications occurred between triangular and trapezoidal waves, due to the fact that both waveforms contain linear variation segments, resulting in local overlap in the feature space. Nevertheless, the proportion of misclassified samples is extremely low, meeting the requirements for engineering applications.

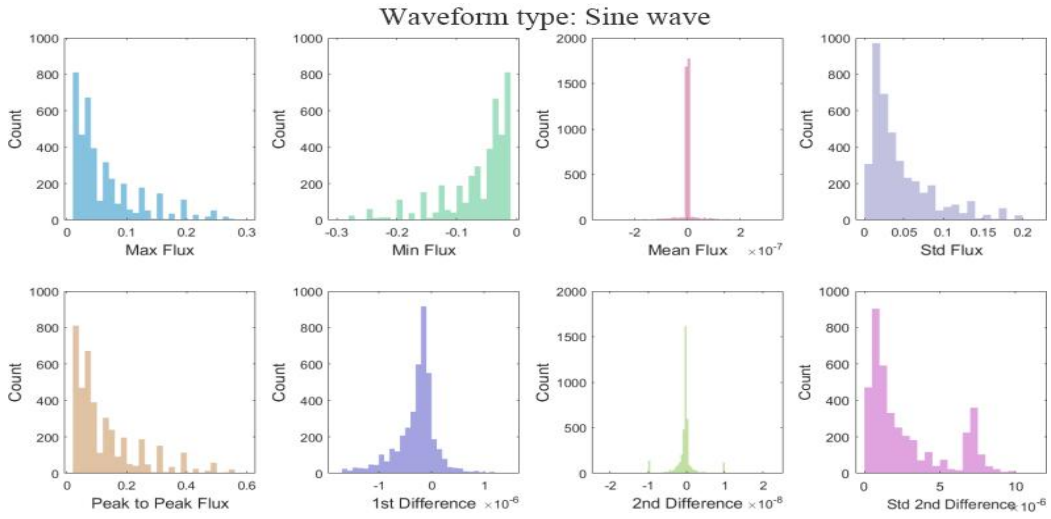

(a) Statistical Analysis of the Magnetic Flux Density of the Sine Wave.

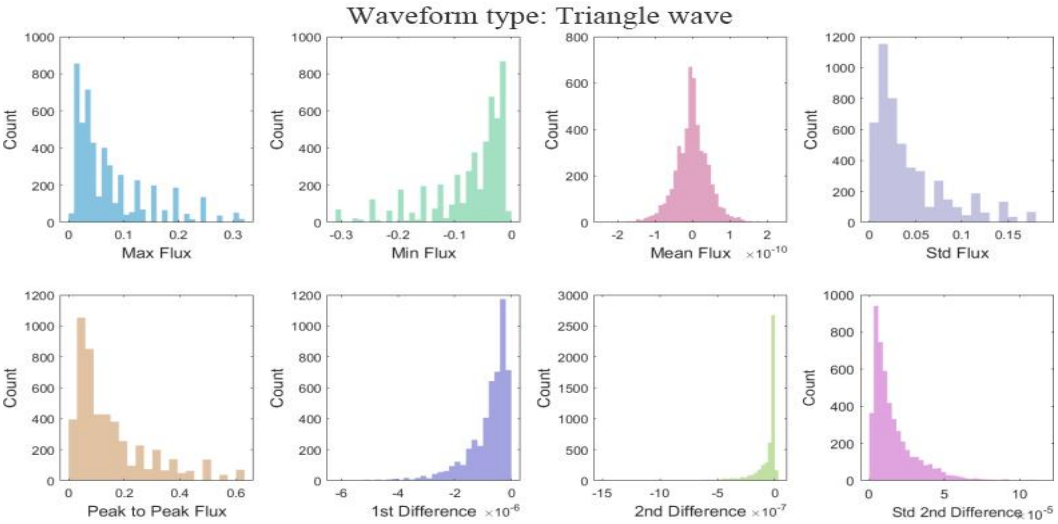

(b) Statistical Analysis of the Magnetic Flux Density of the Triangular Wave.

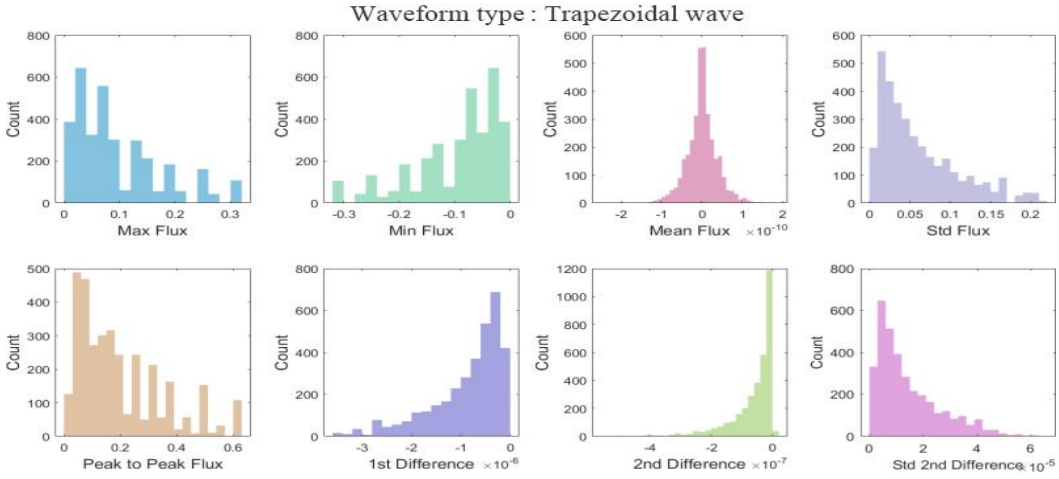

(c) Statistical Analysis of the Magnetic Flux Density of the Trapezoidal Wave.

Fig. 2. Characteristic Statistical Charts of Different Waveforms.

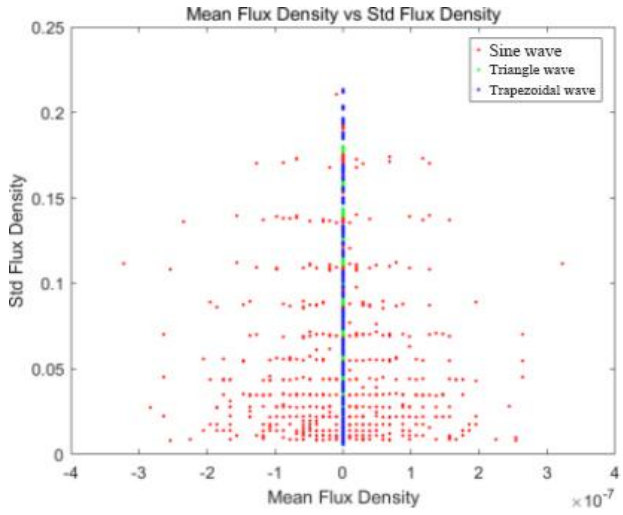

204

205 **Fig. 3.** Average Magnetic Flux Density vs Magnetic Flux Density Standard Deviation.

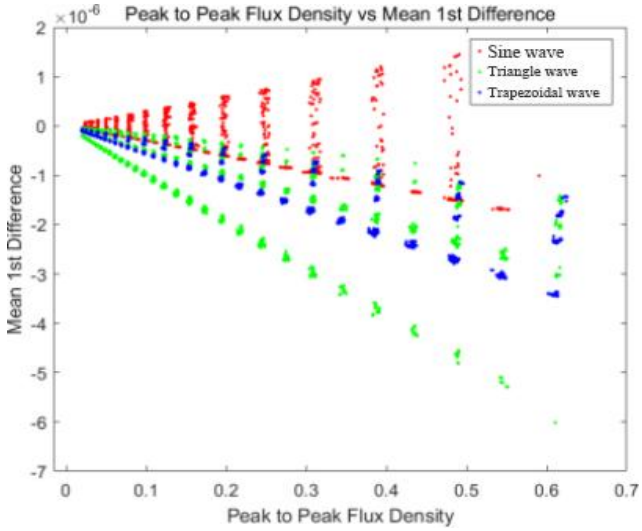

206

207 **Fig. 4.** Average Magnetic Flux Density vs Magnetic Flux Density Standard Deviation.

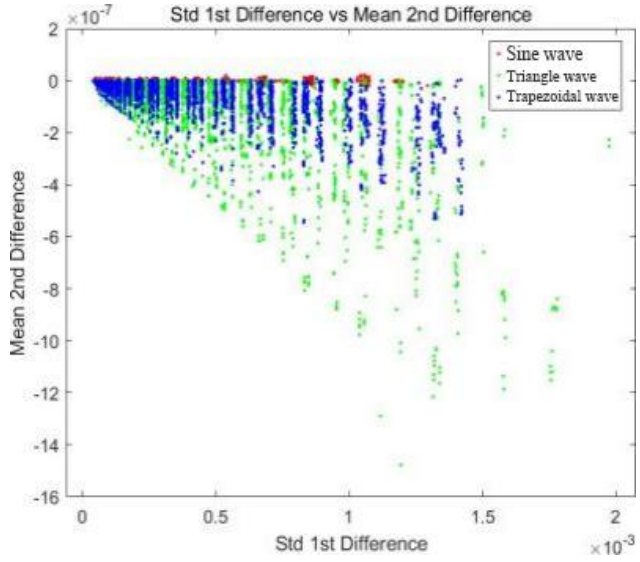

208

209 **Fig. 5** First-order Difference Standard Deviation vs. Second-order Difference Mean.

2.3 Steinmetz Equation Modification Considering Temperature

In traditional magnetic core loss models, the SE is widely used for loss prediction under sinusoidal excitation conditions[25]. Its expression is:

$$P_{loss} = k \cdot f_a \cdot B_{\max}^{\beta} \tag{7}$$

Where P_{loss} represents the core loss, f is the frequency, B_{max} is the peak value of magnetic flux density, and k, α, and β are coefficients obtained by fitting experimental data. Although the Steinmetz equation performs well in certain application scenarios, its predictive accuracy under high-temperature or non-sinusoidal conditions is limited.

To enhance the predictive accuracy of the Steinmetz equation under different temperature conditions, this study modified the equation and developed a new model based on data fitting. By analyzing experimental data, a modified model considering the influence of temperature was proposed. The experimental data were obtained from core loss tests conducted under different temperature conditions, set at 25°C, 50°C, 70°C, and 90°C. First, information such as loss, frequency, and peak magnetic flux density under sinusoidal waveforms was extracted from the experimental data. For sample data at different temperatures, as shown in the **Table 2** below, the values of temperature, frequency, and peak magnetic flux density were calculated, and the loss data under each temperature condition were subjected to statistical analysis.

Table 2. Losses and Parameter Estimates at Different Temperatures

Temperature	Loss	Frequency range	Magnetic flux density peak
25°C	1114.7~1223700	50020~281860	0.0123~0.2731
50°C	739.82~968500	50020~281860	0.0124~0.2730
70°C	684.05~841850	50020~316230	0.0123~0.2734
90°C	708.77~832600	50020~316230	0.0123~0.2738

To better adapt to the loss characteristics at different temperatures, the Steinmetz equation was modified. A polynomial function of temperature, $k(T)$, was introduced, and the revised loss model is:

$$P_{loss} = k(T) \cdot f_a \cdot B_{\max}^{\beta} \tag{8}$$

Where $k(T)$ is a polynomial with respect to the temperature T:

$$k(T) = k_0 + k_1 T + k_2 T^2 + \cdots + k_n T^n \tag{9}$$

We performed polynomial fitting on the experimental data, determined the $k(T)$ coefficients at different orders, and chose the optimal polynomial order n to get the best fitting results.

3. BP-Neural Network Core Loss Prediction Model

The BP-neural Network, with its powerful learning ability and nonlinear mapping capability, can handle prediction tasks for complex systems [26] [27]. The structure of the BP neural network model is shown in **Fig. 6**. The model includes an input layer, two hidden layers, and an output layer. The training of the model is carried out through the backpropagation algorithm. During forward propagation, the input data are processed by the weighted summation and activation functions of neurons at each layer, ultimately producing the predicted output. During error backpropagation, weights and biases are adjusted layer by layer based on the error between the predicted output and the actual value.

The main parameter settings of this BP neural network model are shown in **Table 3**:

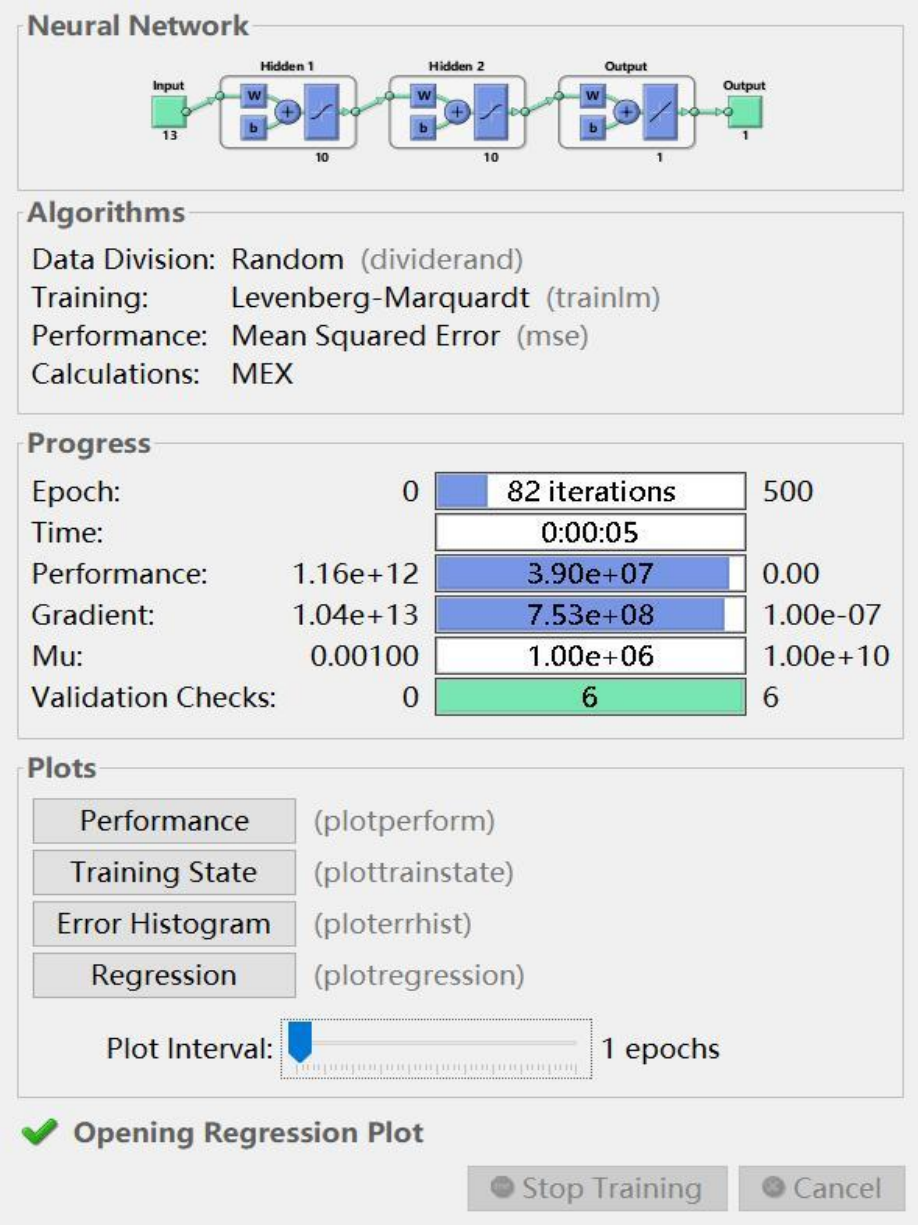

Fig. 6 BP-Neural Network Structure.

Table 3 Main Parameters of the BP-Neural Network Model.

Structural Item	Parameter Value
input layer	12 neurons (corresponding to 12 features)
hidden layer	two layers, with 10 neurons in each layer
output layer	1 neuron
learning rate	0.01
maximum number of iterations	500 times

To construct the optimal model of core loss, the objective function is defined as follows:

$$\min f(x) = P_{loss}(x) + \alpha \cdot (\frac{E_{transfer}(x)}{T}) + \beta \cdot (C_{\omega}(x)) \tag{10}$$

$$E_{transfer}(x) = f \cdot B_{\max} \tag{11}$$

Where $E_{transfer}(x)$ is the transmission of magnetic energy, f is the frequency, B_{max} is the peak magnetic flux density, which $C_{\omega}(x)$ is an indicator of waveform complexity, and α β is the coupling weight coefficient.

The constraint is:

$$f_{\min} \le f \le f_{\max} \tag{12}$$

$$B_{\min} \le B_M \le B_{\max} \tag{13}$$

$$C_{\omega}(x) \le C_{\omega,\max} \tag{14}$$

Using a neural network combined with an improved particle swarm optimization (PSO) algorithm: the neural network is used to predict magnetic core loss Ploss, while the particle swarm algorithm searches for the optimal parameter combination. To determine the weight parameters, this paper designs a greedy algorithm to solve it, with the specific process shown in the table below. The network training process is implemented using the **train** function in MATLAB, which iteratively adjusts the weights and biases using the error backpropagation algorithm.To facilitate the realization of the proposed approach, the necessary procedures are concluded as Algorithm 1.

Algorithm 1: Greedy algorithm determines the coupling weight coefficients α and β.

1: **Initialization**: Set the initial solution to empty and set the initial weights $\boldsymbol{\alpha_0}$, $\boldsymbol{\beta_0}$.
2: **Calculate core loss**: For each pair of weights (α, β), calculate the objective function value $f(\alpha, \beta)$.
3: **Sorting**: Sort all weight combinations according to the objective function value.
4: **for** each weight combination (α_i, β_i) **do.**
5: Choose the currently optimal weight combination and add it to the solution.
6: **if** the current solution satisfies all constraints **then.**
7: Retain the current weight combination in the solution.
8: **else**
9: Remove the current weight combination from the solution.
10: **Check**: If all weight combinations have been considered, continue; otherwise, go back to step 3
11: **Output**: Return the constructed optimal weight solution (α*, β*)

4. Results and Discussion

4.1 Analysis of Classification Results

Random Forest (RF) is an ensemble learning algorithm based on decision trees, whose core idea is to accomplish classification tasks by constructing multiple decision trees [28]. During the training process, each decision tree is independently trained on a subset of the samples, and the final classification result is determined based on a majority voting mechanism. This algorithm has good generalization performance and demonstrates a certain degree of robustness to noisy data, making it suitable for classification problems with complex feature structures. Based on the feature extraction results mentioned above, this study selected the Random Forest classifier as the waveform classification model [29]. This classifier can effectively handle high-dimensional feature data and exhibits superior classification performance. The training and testing datasets were divided in an 80% to 20% ratio. By training the Random Forest classifier, the waveform classification accuracy was obtained. The overall classification accuracy on the test set reached 99.84%, with the sine wave being recognized with high accuracy; trapezoidal waves showed some misclassification due to their similarity in shape to triangular waves. The **table 4** presents the classification accuracy results of the model for different waveform categories.

Table 4 Classification Accuracy.

Classification Accuracy	Precision	Misclassification Rate	Recall	F1-Score
99.84%	100%	0.16%	100%	100%

The confusion matrix results of the random forest model are shown in **Fig. 8**. This matrix intuitively reflects the mapping relationship between the model's predicted results and the true waveform categories of the samples. In the matrix, the columns correspond to the true categories of the samples, while the rows correspond to the predicted categories output by the model. Based on the distribution characteristics of the diagonal and off-diagonal elements of the matrix, one can effectively identify the specific instances of correct classification and misclassification for each

category, thereby providing a quantitative basis for evaluating the classification performance of the random forest model.

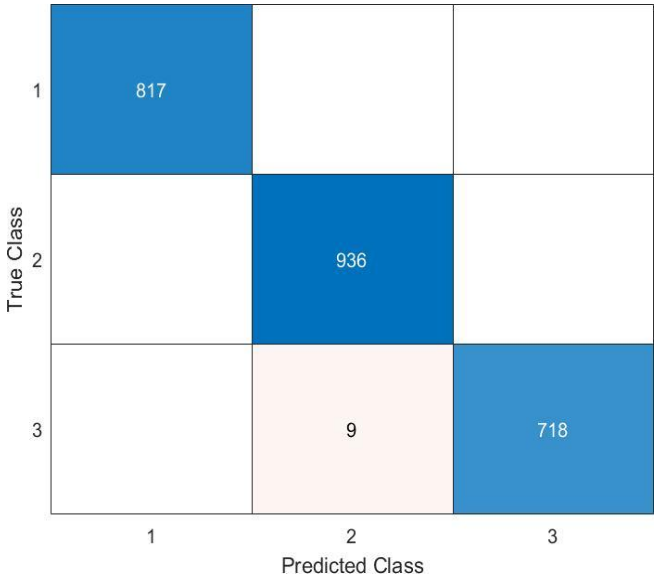

Fig. 7 Confusion Matrix of the Random Forest Model.

As shown in **Fig. 7**, the model performs best in predicting sine waves, while there is a certain misclassification rate for triangular waves due to their similarity with trapezoidal waves; however, the proportion is very small and can be neglected. By extracting various statistical features of the magnetic flux density and combining them with a random forest classifier, an effective waveform recognition model was constructed. Experimental results indicate that the random forest classification model performs excellently in the waveform recognition task, capable of accurately distinguishing different waveform types.

4.2 Model Evaluation and Results Analysis

The model's performance is evaluated using Mean Squared Error (MSE) and R^2. Here's how it performed on the training and test sets is shown in **Fig. 8** below:

As shown in **Fig. 8**, you can see that as the training goes on, the gradients gradually get smaller, showing that the model's loss function is steadily optimizing toward a local minimum. In the figure, the gradients reach a relatively small value at 82 epochs.The MSE curves depict the dynamic changes of MSE on the training, validation, and test sets. As the training depth increases, the MSE of all datasets shows a continuous declining trend, ultimately achieving the optimal MSE on the validation set at the 76th epoch, approximately 41,689,981. The smooth decreasing characteristic of the error curves indicates that the model error continuously converges during the training process and that the predictive performance across different datasets exhibits good consistency.The error histogram shows the error distribution for the training set, validation set, and test set. Most error values are concentrated near zero, indicating that the model's overall predictions are relatively

accurate. These four scatter plots respectively display the comparison between predicted values and true target values for the training set, validation set, test set, and all data. The points in the plots are roughly distributed along the diagonal, indicating a high consistency between the model's predictions and the true values. The corresponding correlation coefficients (R values) are all close to 1, further confirming the model's high precision.

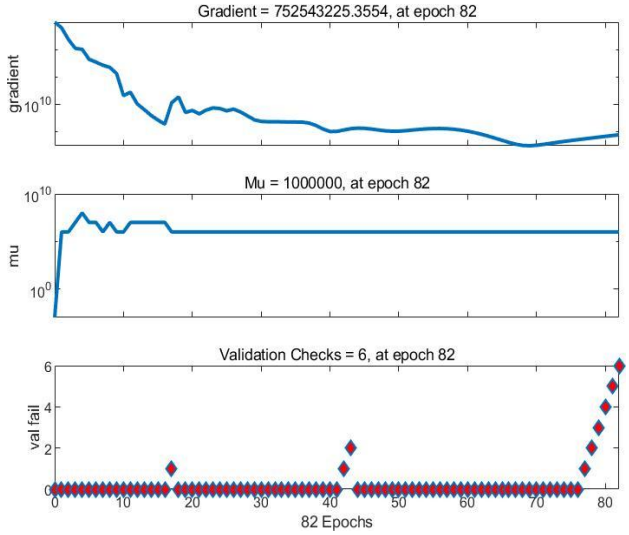

(a) Changes in gradients, Mu parameters, and validation iterations during training.

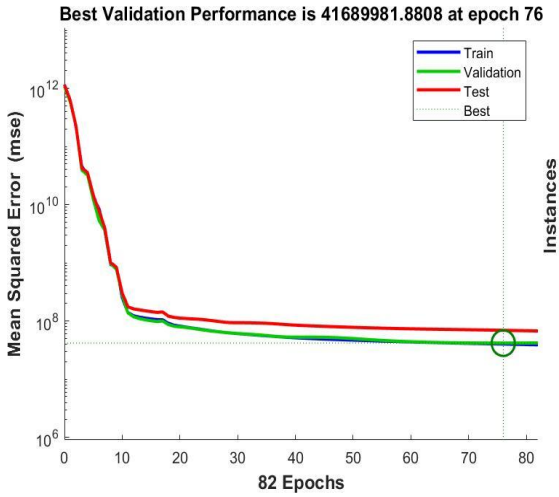

(b) MSE Curve

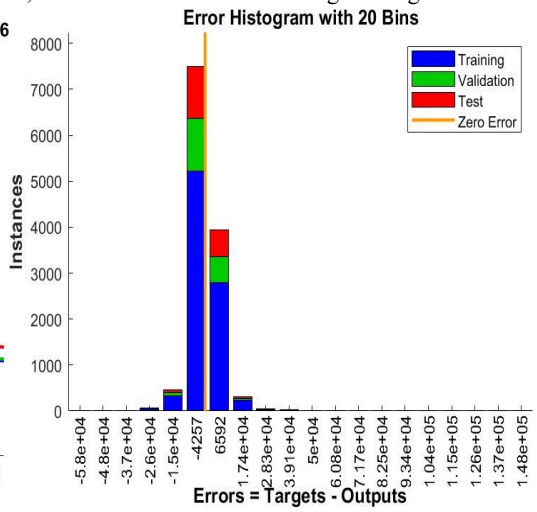

(c) Error Histogram

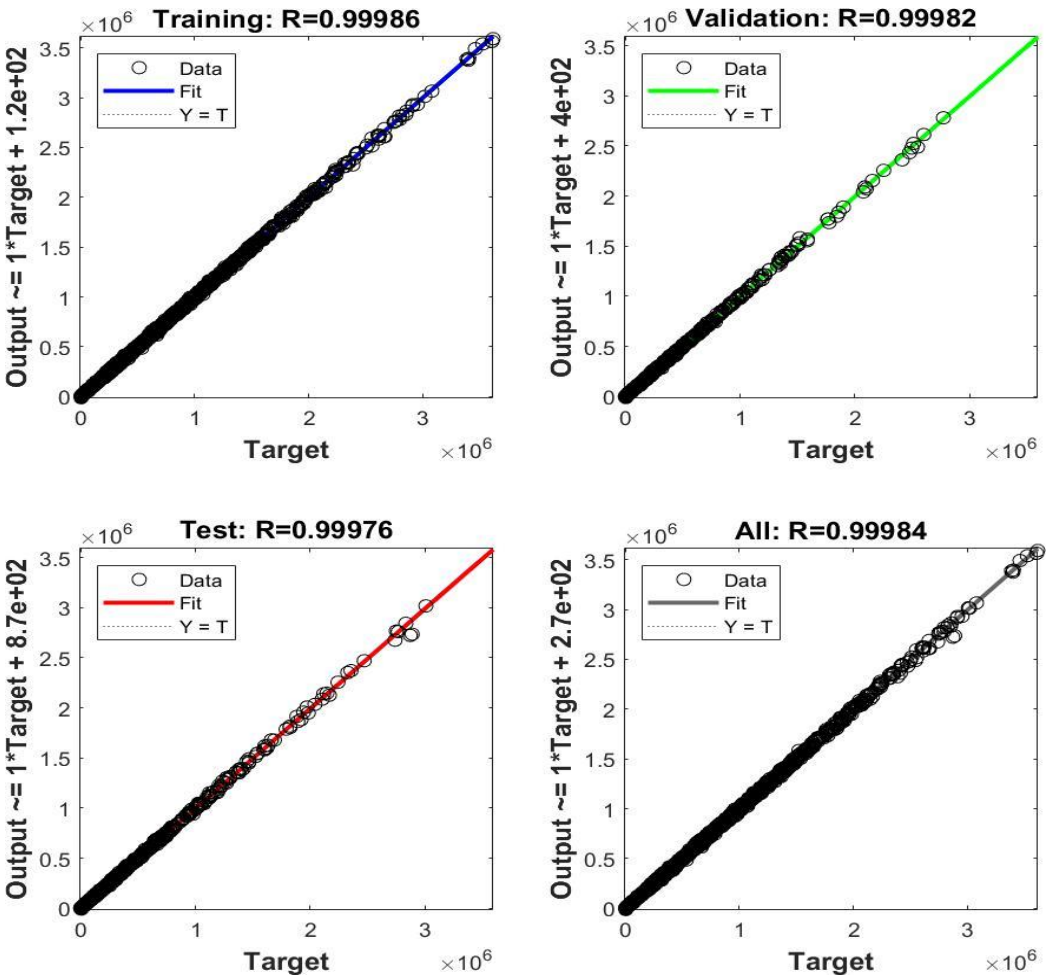

(d)Comparison between output and target

Fig. 8 Model Training and Error Analysis

Fig. 9 is a scatter plot comparing the actual core loss values of the test set with the model's predicted values. The red dashed line in the figure represents the ideal prediction line (**Predicted value = Actual value**).

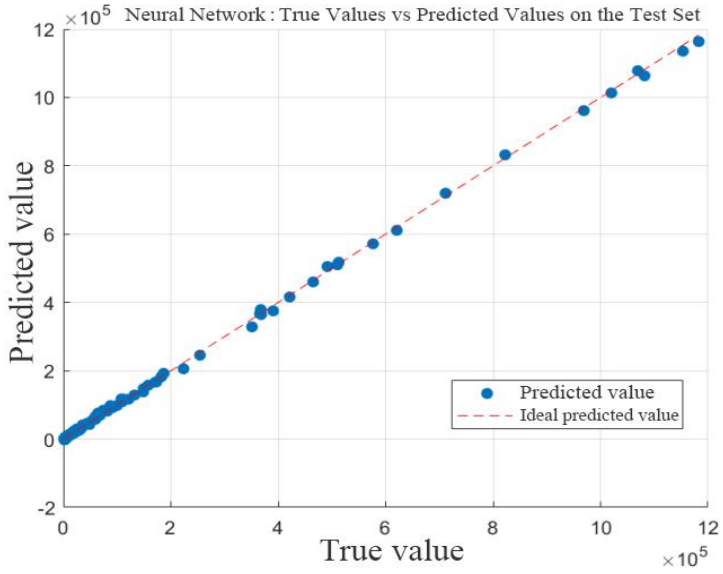

Fig. 9 Scatter Plot of Predicted Values VS. Actual Values.

As observed from the **Fig. 9**, the model's predicted values generally distribute along the ideal diagonal. In the low core loss region, the sample points closely adhere to the ideal curve, indicating that the model achieves good prediction accuracy for low to medium loss conditions. As the loss magnitude increases, the scatter points deviate more from the ideal line, the prediction dispersion becomes larger, and the model's prediction error for high-loss conditions rises.

Fig. 10 shows the residual analysis, further confirming the model's prediction accuracy.

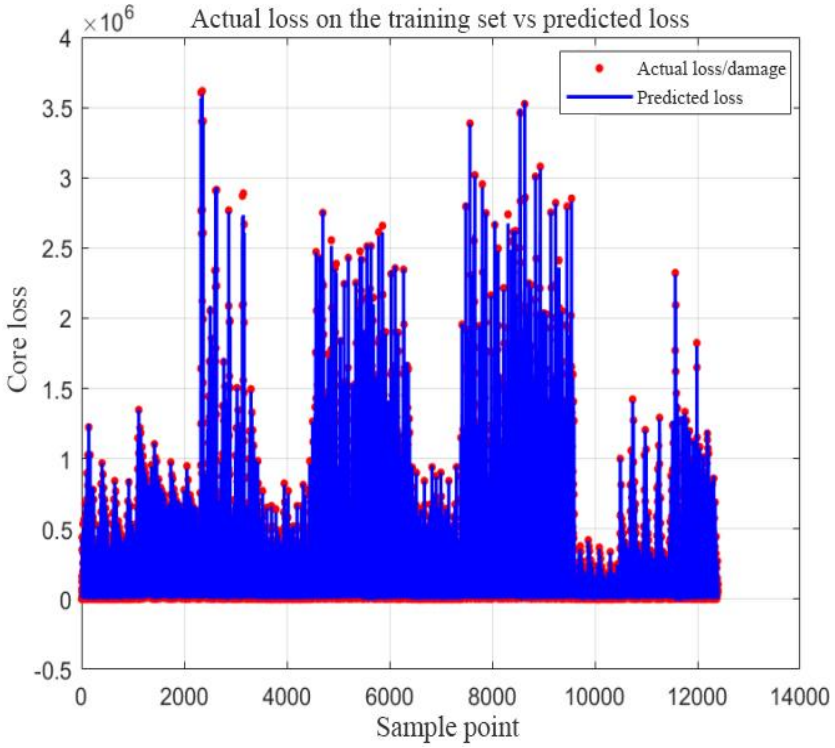

Fig.10 Loss performance on the training set.

As shown in **Fig. 10.** Overall, the model's predicted curve is able to reproduce the general fluctuation trend of core loss with changing operating conditions, and it fits well for the majority of low to medium amplitude losses.

By integrating the results of the two figures, it can be observed that the model has already learned the intrinsic pattern of core loss variation with input operating conditions, demonstrating basic predictive capability. Both the training and testing sets exhibit consistent error characteristics: the fitting performance is good in low-loss regions, while the predictive capability is insufficient under high-loss peak conditions. This phenomenon mainly arises from the uneven distribution of sample amplitudes; the conventional mean squared error loss function tends to prioritize fitting the more abundant medium- and low-loss samples, thereby weakening the learning of the few high-loss extreme samples, and it is not a typical overfitting issue. In the future, methods such as weighted sampling of peak samples, improving the loss function, or optimizing the network structure can be employed to enhance the model's ability to capture high-loss spikes.

5. Conclusion

To address the difficulty in accurately predicting magnetic core losses under multiple excitation waveforms such as sinusoidal, triangular, and trapezoidal waves, varying temperature conditions, and the coupling conditions of various soft magnetic materials, this paper proposes a data-driven method for magnetic core loss prediction and multi-condition optimization modeling. Firstly, the time-domain statistical features and differential features of magnetic flux density are extracted, and the random forest algorithm is used to achieve intelligent recognition of the three types of excitation waveforms. Secondly, a temperature polynomial is introduced to modify the Steinmetz equation, and a BP neural network surrogate model is constructed to achieve high-precision prediction of magnetic core loss. Finally, the trained neural network model is coupled with an improved particle swarm optimization algorithm, with the objectives of minimizing magnetic core loss and maximizing transmitted magnetic energy, to perform parameter optimization under multi-objective constraints. The results show that: the random forest classification model constructed based on the statistical and differential features of magnetic flux density can effectively identify sinusoidal, triangular, and trapezoidal waveforms, achieving an overall recognition accuracy of 99.84%; the Steinmetz equation with a quadratic polynomial temperature correction term has a fitting goodness R^2 of 0.9908, significantly improving its loss prediction capability under varying temperature conditions compared to the original model; the BP-Neural Network model has a fitting goodness R^2 of 0.9982 and MSE of 134,018.16 on the test set; after coupling with the improved particle swarm optimization algorithm, the optimal parameter combination is obtained that balances low magnetic core loss with high transmitted magnetic energy. The results of this study provide theoretical reference value for the evaluation of magnetic component losses and the optimization of operating condition parameters.

References

[1] Liu Y F, Tan D. A discussion on ultrahigh efficiency and ultrahigh power density DC-DC converter technologies[J]. IEEE Journal of Emerging and Selected Topics in Power Electronics, 2023,11(3): 2457-2468.

[2] Qida Y, Peng Y, Xinyi Z, et al. A Machine Learning-Based Method for Predicting Core Loss in Magnetic Components[J]. Journal of Nantong University (Natural Science Edition), 2025, 24(2):29-38.

[3] Safayatullah M, Elrais M T, Ghosh S, et al. A comprehensive review of power converter topologies and control methods for electric vehicle fast charging applications[J]. IEEE Access, 2022, 10:40753-40793.

[4] Liu S , Li T , Luo J ,et al.Core Loss Analysis of Soft Magnetic Composites Based on 3D Model Considering Temperature Influence[J].IEEE Access, 2021, PP(99):1-1.

[5] Kuang Jianjun, Zheng Lixin, Lu Xiaofen, et al. Calculation of Core Loss under Non-Sinusoidal Excitation[J]. Magnetic Materials and Devices, 2009, 40(1):3.

[6] Ye Jianying, Chen Wei, Wang Jinghui. Study on Core Loss Model under PWM Wave and DC Bias Excitation[J]. Proceedings of the Chinese Society for Electrical Engineering, 2015, 35(10): 2601-2606.

[7] Chengguang O, Pengxiang Z, Jiashuo Y. Analysis of Magnetic Core Loss in Magnetic Components Based on Data-Driven Methods [J]. Practice and Understanding of Mathematics, 2025, 55(10):79-91.

[8] Han X, Yang F, Chen H, et al. Experimental investigation on the hysteresis characteristic of vacuum arc voltage during the current commutation[J]. Vacuum, 2025, 238: 114211.

[9] Yin B, Jiao X, Fang Y, et al. Dynamic viscoelasticity and hystere sis loss of carbon black filled rubber: measurements and prediction [J]. Polymer Composites, 2025, 46(S1): 132-141.

[10] Bertotti Giorgio. General properties of power losses in soft ferromagnetic materials[J]. IEEE Trans Magn, 1988, 24(1): 621-630.

[11] Kunecky' J, Štembera V, Kloiber M, et al. Optimization of CZM parameters of Norway spruce tested in mode I using multistart sim plex method[J]. Engineering Fracture Mechanics, 2024, 310: 110430.

[12] Daniela S R, Rodriguez-Licea M A, Soriano-Sanchez A G, et al. Advanced ferromagnetic materials in power electronic converters: a state of the art[J]. IEEE Access, 2020, 8: 56238-56252.

[13] Li, J.; Abdallah, T.; Sullivan, C.R. Improved calculation of core loss with nonsinusoidal waveforms. In Conference Record of the 2001 IEEE Industry Applications Conference; 36th IAS Annual Meeting (Cat. No. 01CH37248); IEEE: New York, NY, USA, 2001; Volume 4, pp. 2203–2210.

[14] Venkatachalam, K.; Sullivan, C.R.; Abdallah, T.; Tacca, H. Accurate prediction of ferrite core loss with nonsinusoidal waveforms using only steinmetz parameters. In 2002 IEEE Workshop on Computers in Power Electronics; IEEE: New York, NY, USA, 2002; pp. 36–41.

[15] Arruti, A.; Anzola, J.; Pérez-Cebolla, F.J.; Aizpuru, I.; Mazuela, M. The composite improved generalized steinmetz equation (ciGSE): An accurate model combining the composite waveform hypothesis with classical approaches. IEEE Trans. Power Electron. 2023, 39, 1162–1173.

[16] Shuai Chunyan, Meng Defen, Zhang Xiaoqi, et al. Magnetic Core Loss Prediction Based on Data-Driven and Improved Steinmetz Equation [J]. Science Technology and Engineering, 2026, 26(8): 3330-3337.

[17] Wang Ning, Zhang Pengning, Miao Dengji, et al. Research on the Steinmetz loss model of nanocrystalline materials under variable temperature conditions[J]. High Voltage Technology, 2025, 51 (11): 5673-5682.

[18] He,J.; Wei, Y.; Jin, D. Modeling of Core Loss Based on Machine Learning and Deep Learning. arXiv 2025, arXiv:2502.05487.

[19] Deng,J.; Wang, W.; Ning, Z.; Venugopal, P.; Popovic, J.; Rietveld, G. High-frequency core loss modeling based on knowledge aware artificial neural network. IEEE Trans. Power Electron. 2023, 39, 1968–1973.

[20] Solimene, L.; Ragusa, C.S.; Giuffrida, A.; Lombardo, N.; Marmello, F.; Morra, S.; Pasquale, M. A hybrid data-driven approach in magnetic core loss modeling for power electronics applications. In 2024 IEEE 22nd Mediterranean Electrotechnical Conference (MELECON); IEEE: New York, NY, USA, 2024; pp. 1356–1361.

[21] Shen, X.; Wouters, H.; Martinez, W. Deep neural network for magnetic core loss estimation using the magnet experimental database. In 2022 24th European Conference on Power Electronics and Applications (EPE'22 ECCE Europe); IEEE: New York, NY, USA, 2022; pp. 1–8.

[22] Brendel, P.; Medvedev, V.; Roßkopf, A. Convolutional Physics-Informed Neural Networks for Fast Prediction of Core Losses in Axisymmetric Transformers. IEEE Transaction Magnetics. 2024, 60, 7201704.

[23] Luo Pengyong, Huang Xiaosheng, Lin Shuyi, et al. A Method for Predicting Ferrite Core Loss Based on TCN and Attention Mechanism [J/OL]. Journal of Power Supply, 2026, 10, 1-14.

[24] Barg S, Bertilsson K. Core loss modeling and calculation for trapezoidal magnetic flux density waveform[J]. IEEE Transactions on Industrial Electronics, 2020, 68(9): 7975-7984.

[25] Lu C, Meng F, Zhang J, et al. Core Loss Prediction Model of High-Frequency Sinusoidal Excitation Based on Artificial Neural Network[J]. Magnetochemistry, 2025, 11(11): 93.

[26] Li J, Cheng J, Shi J, et al. Brief introduction of back propagation (BP) neural network algorithm and its

433 improvement[M]//Advances in computer science and information engineering: volume 2. Berlin, Heidelberg:
434 Springer Berlin Heidelberg, 2012: 553-558.
435 [27]Jin W, Li Z J, Wei L S, et al. The improvements of BP neural network learning algorithm[C]//WCC 2000-ICSP
436 2000. 2000 5th international conference on signal processing proceedings. 16th world computer congress 2000.
437 IEEE, 2000, 3: 1647-1649.
438 [28]Liu Y, Wang Y, Zhang J. New machine learning algorithm: Random forest[C]//International conference on
439 information computing and applications. Berlin, Heidelberg: Springer Berlin Heidelberg, 2012: 246-252.
440 [29]Ghiasi M M, Zendehboudi S. Application of decision tree-based ensemble learning in the classification of breast
441 cancer[J]. Computers in biology and medicine, 2021, 128: 104089.